SAND2018-6424C

TERRY TURBINE EXPANDED OPERATING BAND: SANDIA NATIONAL LABORATORIES TERRY TURBINE ANALYTICAL EFFORTS

J. Cardoni, K. Ross, B. Beeny, and D. Osborn
Sandia National Laboratories*
P.O. Box 5800
Albuquerque, NM 87185-0748
jncardo@sandia.gov; kwross@sandia.gov; babeeny@sandia.gov; dosborn@sandia.gov

ABSTRACT

The paper details the computational fluid dynamic and system-level modeling, including a mechanistic representation of a Terry turbine/pump, for Fukushima Daiichi Unit 2. Until this recent effort, mechanistic modeling had been confined to an otherwise coarse model of Fukushima Daiichi Unit 2 laden with manipulations of boundary conditions that substituted for detailed representations of the reactor, drywell, and wetwell. This work has provided insights in modeling uncertainties and provides confirmation for experimental efforts for the Terry turbopump. Analytical efforts ongoing at Sandia National Laboratories to understand the design and off-design operation of Terry turbines are introduced in this paper. The efforts are described mostly in the context of RCIC systems.

KEYWORDS
Terry turbine, RCIC, Fukushima, TDAFW

1. INTRODUCTION

Turbine driven pumps at nuclear power plants are propelled by steam produced from heat generated by the radioactive decay of fission products in the reactor that it serves. A turbine driven pump serving a pressurized water reactor (PWR) is termed a turbine-driven auxiliary feedwater (TDAFW) pump while one serving a boiler water reactor (BWR) is termed a reactor core isolation cooling (RCIC) pump. Turbine driven pumps are important to the normal operation of a nuclear power plant and to beyond design basis event operations as exemplified by the Fukushima Daiichi Unit 2 accident progression where the RCIC pump managed to cool the reactor for some 70 hours given a complete loss of all electrical power and no operator intervention [1]. Considering the extended cooling provided in adverse conditions at Unit 2, a turbine (specifically a Terry turbine) driven pump is notionally a resilient self-regulating piece of equipment that can be counted upon in a beyond design basis event, even one with an extended loss of all electrical power, to remove decay heat until external pumps, portable generators, etc., can be deployed to ultimately stabilize the plant. Detailed understanding of Terry turbine design and off-design response is necessary to develop confidence in this perceived benefit. Specifically, understanding Terry turbine response under off-design conditions hinges upon analytically and experimentally derived explanations. The analytical efforts are being informed by complementary experimental efforts described in a companion paper [2].

---

* Sandia National Laboratories is a multi-mission laboratory managed and operated by National Technology & Engineering Solutions of Sandia, LLC, a wholly owned subsidiary of Honeywell International Inc., for the U.S. Department of Energy's National Nuclear Security Administration under contract DE-NA0003525. This paper describes objective technical results and analysis. Any subjective views or opinions that might be expressed in the paper do not necessarily represent the views of the U.S. Department of Energy or the United States Government. SAND2018-XXXX

2. RCIC OVERVIEW

A RCIC pump is a steam turbine-driven pump that provides makeup water to the reactor pressure vessel (RPV) of a BWR following core isolation events. The turbine receives steam from the RPV, via relatively small steam piping that taps into a main steam line (MSL), and drives a pump by means of a common shaft. The pump may take suction from the condensate storage tank (CST) or from the wetwell of the containment. The turbine discharges steam to the wetwell.

The turbine in the RCIC system is a small, single-stage, compound-velocity, impulse turbine that was originally designed and manufactured by the Terry Steam Turbine Company, which was later purchased by Ingersoll-Rand in 1974, and are currently marketed by Dresser-Rand. The turbine is essentially a solid cylindrical wheel with several semi-circular 'buckets' that are shaped into the body of the wheel. All Terry applications in the US use a "G turbine frame size" that denotes a 24 inch (0.61 m) diameter turbine wheel with fixed nozzles and reversing chambers that surround the wheel inside the turbine casing. Figure 1 illustrates the geometry and flow path of steam through the nozzle, turbine buckets, and reversing chambers.

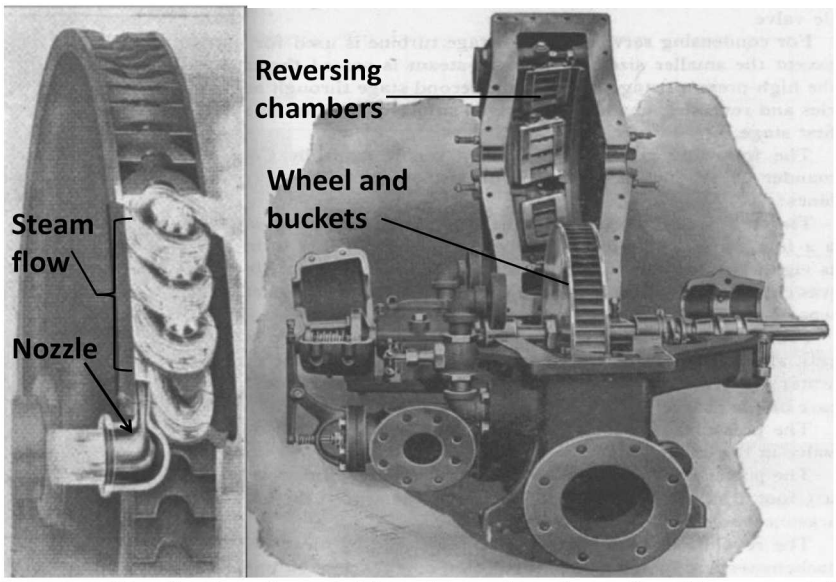

Figure 1. Terry turbine bucket flow (left) and interior view of turbine case (right) [3][4]

Steam enters the semi-circular buckets after expanding through five to ten nozzles that are fixed around the wheel; steam flow direction is reversed 180° in the buckets. The nozzles are separated by at least three buckets to make room for reversing chambers that also surround the wheel. Since the steam is (almost) completely expanded after exiting the nozzles, which are fixed and detached from the turbine wheel, the expansion process itself imparts no energy on the turbine. For this reason, the pressure drop and the enthalpy change over the RCIC turbine are essentially zero. This is in direct contrast to the operation of a reaction turbine (e.g., main turbine) where steam expands in the turbine blades, and the blades themselves act as nozzles. Hence, the typical formulas and relationships for multi-stage reaction turbines are not valid for mechanistic analyses of RCIC turbines. Being a pure impulse turbine, RCIC principally operates on the exchange of momentum and kinetic energy. Turbine motion is induced by means of steam acceleration in the buckets after it has been totally expanded through the nozzles.

The compound-velocity feature of the Terry design refers to the fixed reversing chambers that redirect ejected steam back into the buckets several times. The intent is to capture as much of the steam's kinetic energy as possible.

3. MOMENT-OF-MOMENTUM CONSIDERATION OF TERRY TURBINE OPERATION

Figure 2 illustrates the interaction of a steam jet and a Terry turbine wheel.

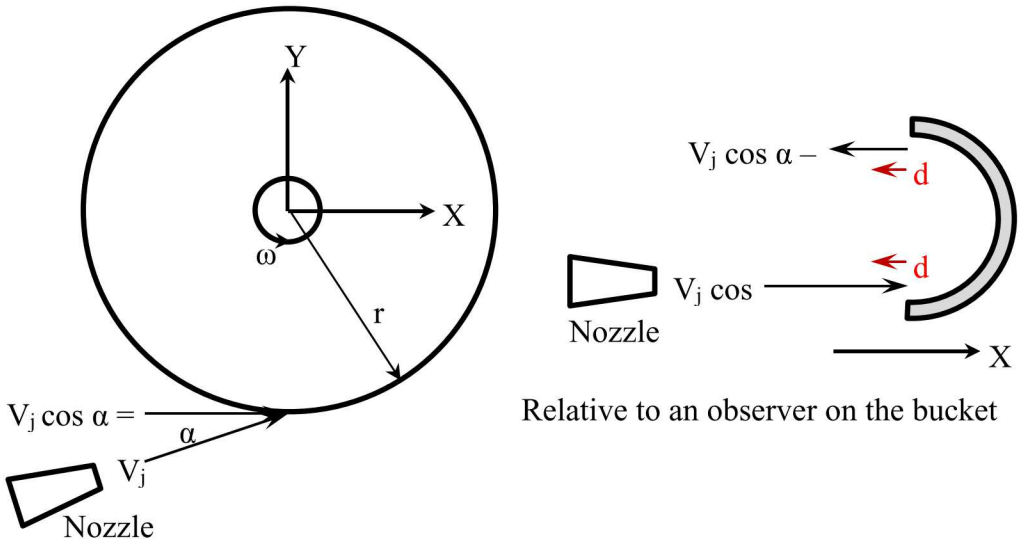

Figure 2. Interaction Between a Steam Jet and a Terry Turbine Wheel

Considering the moment-of-momentum equation for an inertial control volume is Eq. (1)

$$\oiint_{CS} \boldsymbol{r} \times \boldsymbol{T}\, dA + \iiint_{CV} \boldsymbol{r} \times \boldsymbol{B}\, dv = \oiint_{CS} (\boldsymbol{r} \times \boldsymbol{V})(\rho \boldsymbol{V} \cdot d\boldsymbol{A}) + \frac{\partial}{\partial t} \iiint_{CV} (\boldsymbol{r} \times \boldsymbol{V})(\rho\, dv) \tag{1}$$

and the scalar component of the same, where

- **r** X **T** is replaced by $\overline{r}$ Tθ
- **r** X **B** is replaced by $\overline{r}$ Bθ
- **r** X **V** is replaced by $\overline{r}$ V_θ

and where

- $\overline{r}$ is the distance from the axis of rotation to the periphery of the turbine wheel
- Tθ , Bθ , and Vθ are tangent to the wheel and in a plane normal to the axis of rotation

This yields Eq. (2)

$$\oiint_{CS} \overline{r} T_\theta\, dA + \iiint_{CV} \overline{r}\, B_\theta\, dv = \iint_{CS} (\overline{r}\, V_\theta)(\rho \boldsymbol{V} \cdot d\boldsymbol{A}) + \frac{\partial}{\partial t} \iiint_{CV} (\overline{r}\, V_\theta)(\rho\, dv) \tag{2}$$

The 1st term on the right side of this equation embodies the moment of momentum flow terms that relate to the torque developed by the jet on the turbine wheel. The terms form as Eq. (3)

$$-Torque = r(V_i \cos\alpha)(-\rho_i V_i A_i) + r[-(V_o \cos\alpha - \omega r) + \omega r](\rho_o V_o A_o) \tag{3}$$

V_o and V_i differ due to spreading of the jet as it traverses a bucket. Of special note in this equation is the relationship for the velocity exiting the bucket relative to the ground given by Eq. (4)

$$-(V_o \cos\alpha - \omega r) + \omega r \tag{4}$$

This relationship is not especially straightforward to recognize. From continuity, Eq. (5) is derived

$$\dot{m} = \rho_i V_i A_i = \rho_o V_o A_o \tag{5}$$

Substituting, yields Eq. (6)

$$-Torque = r(V_i \cos\alpha)(-\dot{m}) + r[-(V_o \cos\alpha - \omega r) + \omega r](\dot{m}) \tag{6}$$

Considering the torque developed by a water jet, velocity is limited to the throat velocity as the jet would be incompressible for Eq. (7)

$$Torque_{water} = 2r\dot{m}_{water}\left(V_{throat,water} \cos\alpha - \omega r\right) \tag{7}$$

Note that if the velocity of the water jet is lower than the tangential velocity of the turbine wheel (i.e., lower than the velocity of the buckets), this relationship becomes invalid as the jet would not be driving the wheel. The torque developed by steam and water jetting together from the steam nozzles to the turbine buckets is taken to be the sum of the torques produced by the steam and water individually. This drive torque is balanced against pump resistive torque to determine system speed.

V_i and V_o are quantities that system-level thermal-hydraulic codes (e.g., SNL's MELCOR code) cannot determine. Commercially available computational fluid dynamics (CFD) codes, however, can describe the supersonic expansion of a condensing steam jet (such as a RCIC turbine steam jet) believably if thoughtfully applied. CFD has been used as presented in Section 4 to quantify V_i and V_o.

4. CFD APPLICATION TO A TERRY TURBINE

The CFD work initiated with a computer-aided drafting (CAD) effort that constructed representations of Terry turbine geometry for use in the CFD applications. Accomplishments of the CAD efforts are exemplified in Figure 3 and Figure 4 [5].

The FLUENT code was used in SNL's CFD Terry turbine modeling [5] [6] [7]. The FLUENT model used is illustrated in Figure 5. Mesh size (depicted in Figure 6) and CPU time is reduced by modeling just a wedge of a turbine. The interior of the turbine, which includes the wheel and buckets, is in a separate domain from the nozzles, reversing chambers, and turbine casing wall. This will enable future calculations of moving reference frames to simulate turbine rotation. The angular speed of the turbine likely has important effects on the bucket exit velocity and the efficacy of the reversing chambers.

Inlet and outlet surfaces were defined for the Terry buckets in order to extract the most representative values from the velocity field calculated using FLUENT. Figure 7 shows the definition of the bucket inlet and outlet surfaces. Velocity magnitudes for the system model were integrated (averaged) over these surfaces. Note that SNL Terry turbine CFD calculations to date are steady-state with the turbine wheel as stationary (representative of the turbine at startup or low speed). Relative movement between the nozzle and buckets should not drastically affect the bucket inlet flow, but it will probably have an influence on the bucket outflow and will be examined in future CFD analyses.

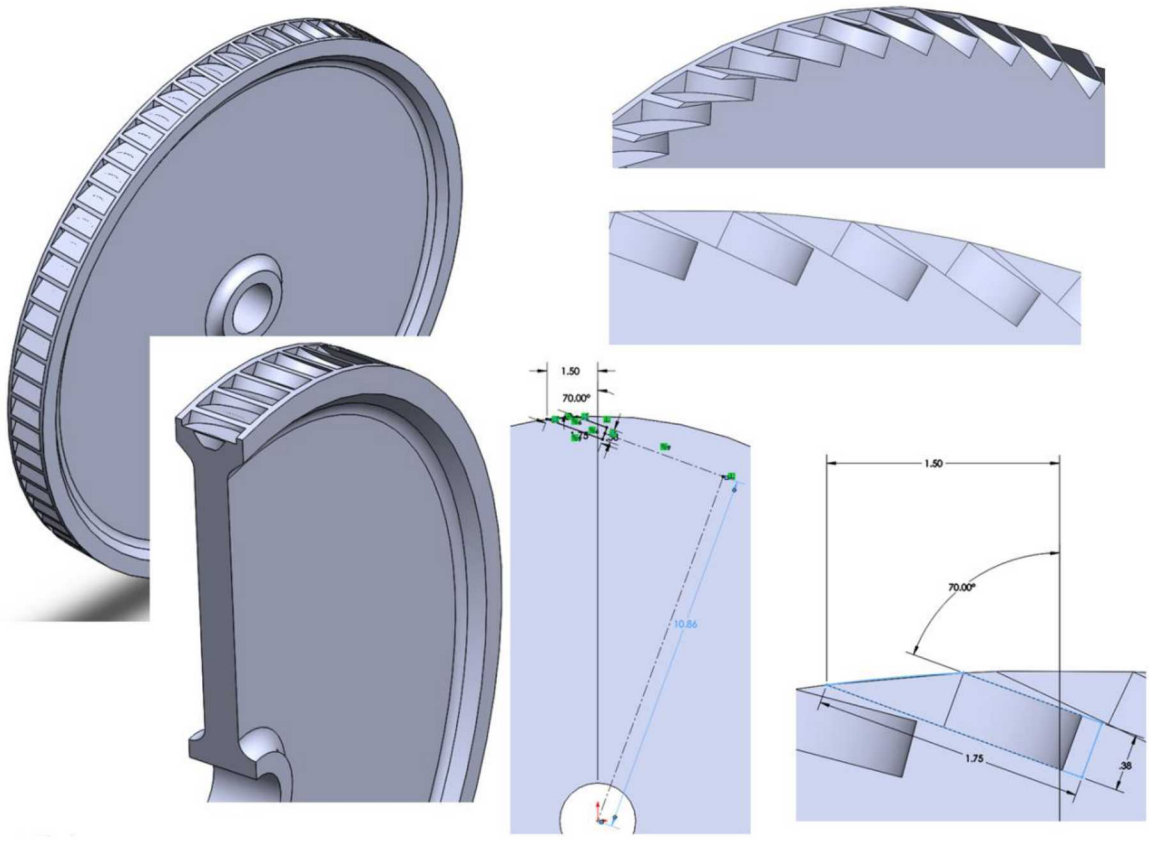

Figure 3. CAD Model of a Terry Turbine Wheel

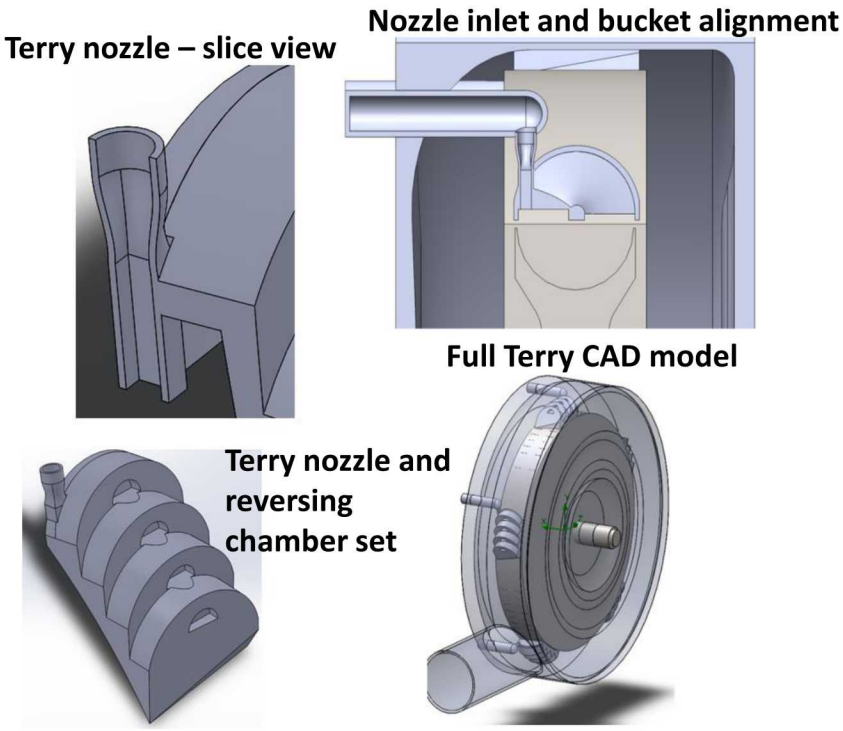

Figure 4. CAD Depictions of a Terry Turbine Nozzle, Reversing Chamber, and Bucket Orientation

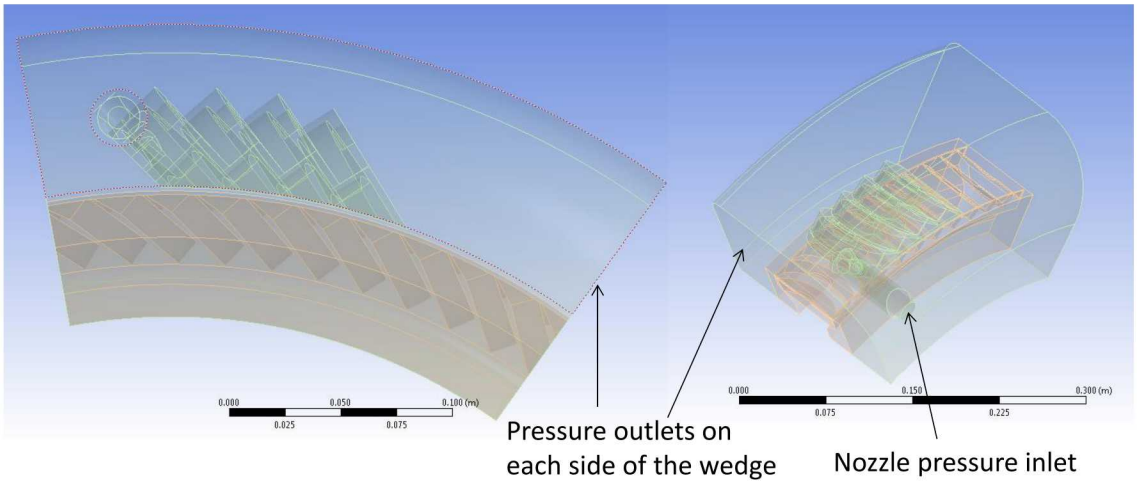

Figure 5. Wedge of Terry Turbine Used in FLUENT Assessments of Nozzle Flow

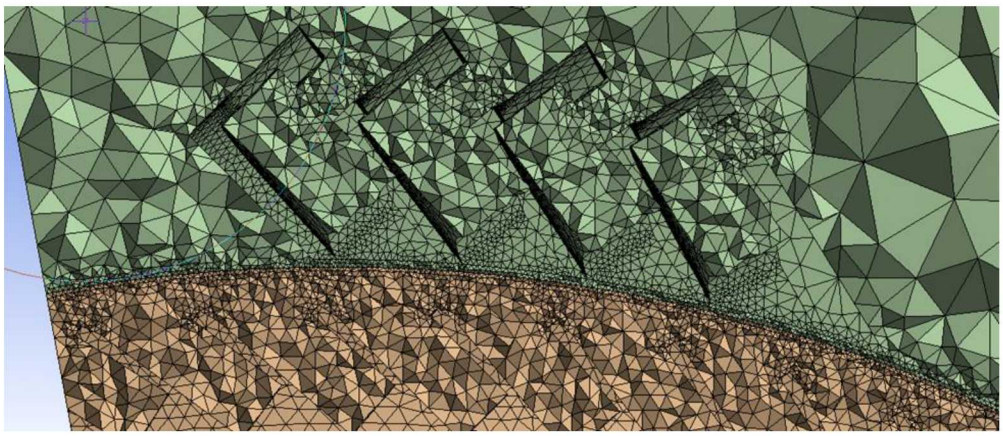

Figure 6. FLUENT Mesh of Wedge Model for Terry Turbine

The nozzle-bucket alignment is intended to approximately simulate the average flow behavior of a moving turbine and the bucket thickness is comparable to the jet width (most of the time the flow is split between two adjacent buckets). The FLUENT model assumes a split of about 25/75 flow between two buckets, as shown in Figure 7.

FLUENT calculations were executed for the reduced Terry model for 11 inlet pressures and 2 outlet pressures. Logarithmic fits to the bucket inlet and outlet velocities as a function of nozzle pressure ratio (P_{in}/P_{out}) are shown in Figure 8 and Figure 9, respectively; larger pressure drops yielded higher velocities. Higher inlet pressure obviously increases the density and available enthalpy of the inlet fluid, which allows for more expansion of the fluid through the nozzle and greater kinetic energy generation. The independent influence of the outlet pressure is slightly counterintuitive, given that outlet pressure cannot affect the mass flow rate due to choked flow. Nevertheless, FLUENT consistently predicts that lower outlet pressure can increase the nozzle and bucket velocities without changing the flow rate through the nozzle.

Flow contours through the nozzle midplane illustrate the effects that inlet and outlet pressures have on the developed velocity field and liquid fraction through the turbine. Figure 10 shows contours of the velocity magnitude for an inlet pressure of 750 psia and an outlet pressure of 44 psia.

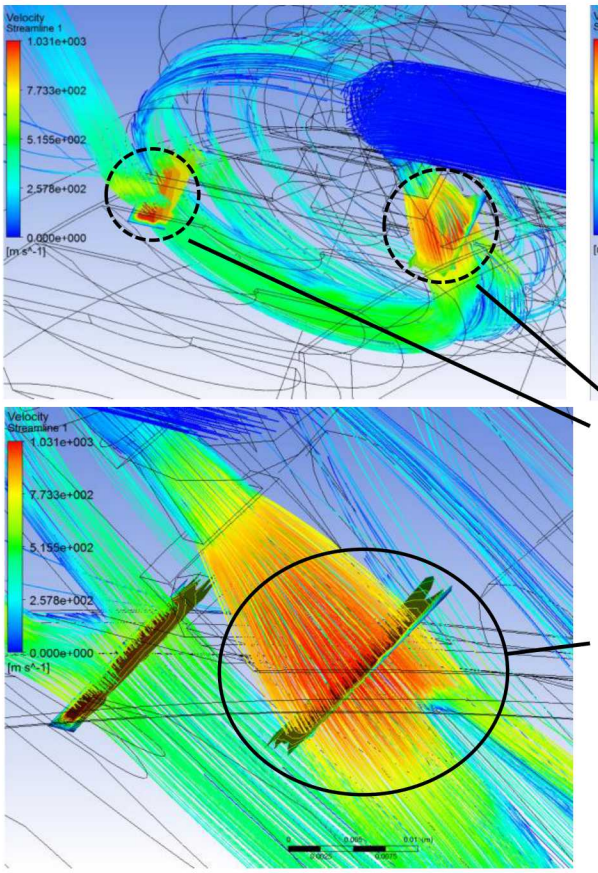

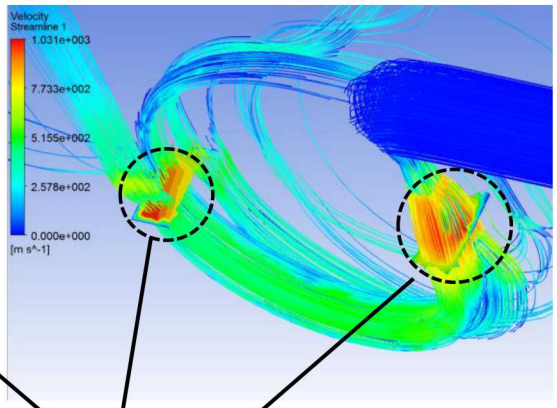

Define bucket inlet and outlet surfaces

Surfaces are perpendicular to the outlet plane of the nozzle; flow is predominately perpendicular to these surfaces.

Fluent calculations are steady and static – the bucket is not moving. This represents the turbine at startup or low speed. The bucket flow is aligned such that there is a split in flow between two adjacent buckets (~75/25 split); most of the time, flow is being split between two buckets since the nozzle jet width is comparable to bucket width.

A moving bucket would probably have some influence on the outlet velocity, but would not directly affect the bucket inlet velocity

Figure 7. Definition of Bucket Inlet and Outlet Surfaces

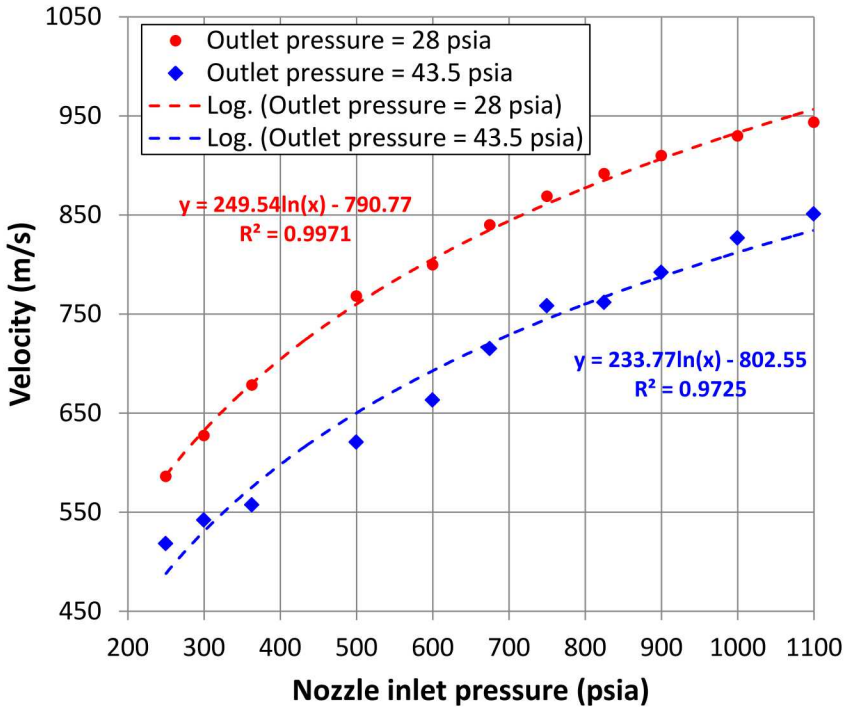

Figure 8. Bucket Inlet Velocity as a Function of Pressure

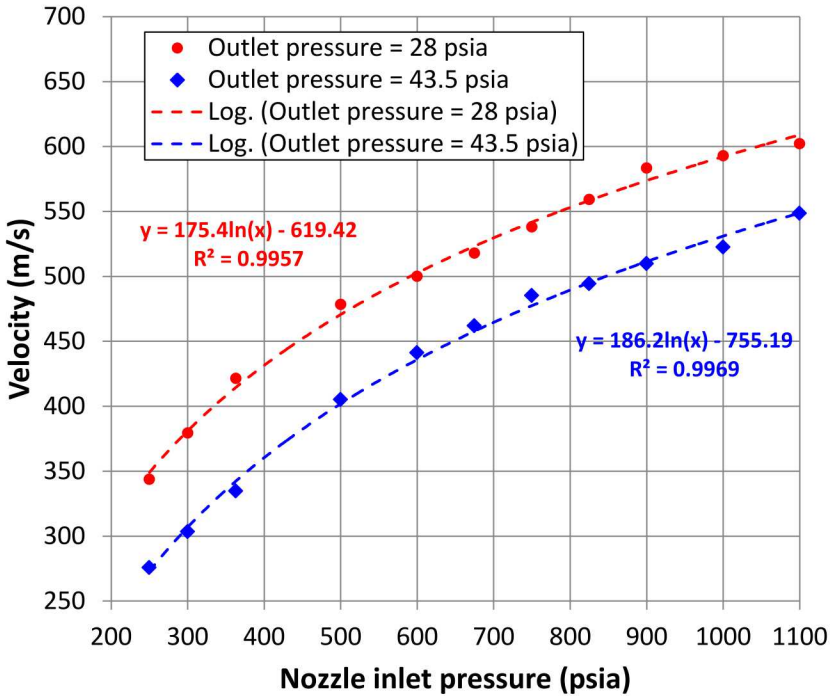

Figure 9. Bucket Outlet Velocity as a Function of Pressure

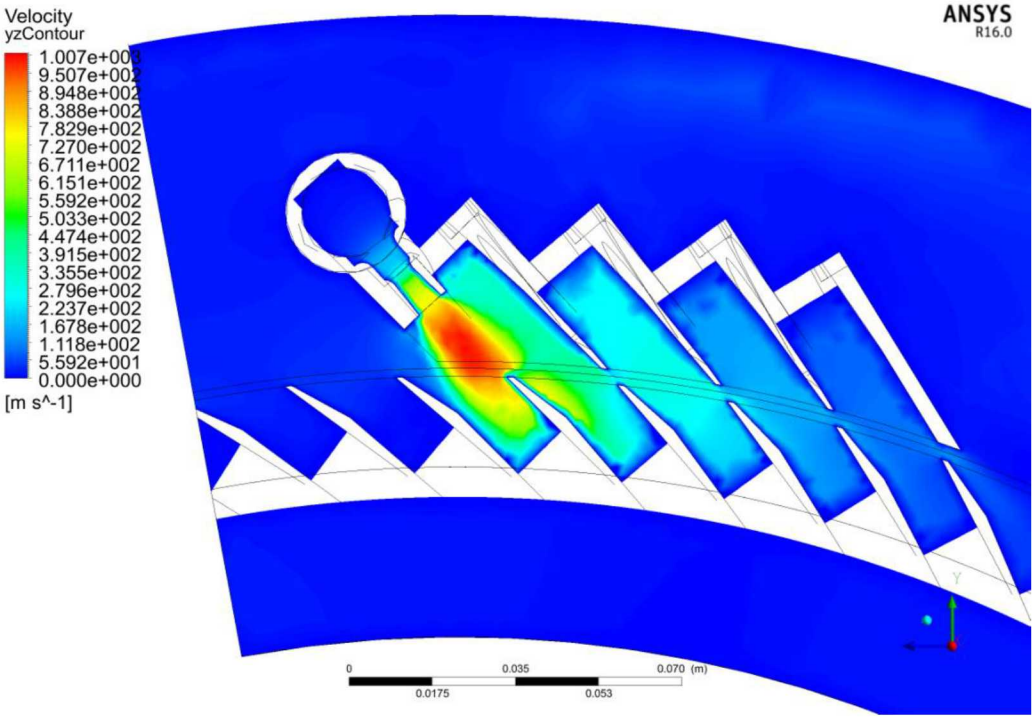

Figure 10. Velocity Field for 750 psia to 44 psia Pressure Drop

5. MODELING OF FUKUSHIMA DAIICHI UNIT 2 RCIC SYSTEM RESPONSE

A MELCOR model with a full representation of the Fukushima Daiichi Unit 2 reactor, reactor vessel, containment, reactor building and RCIC turbine/pump system is being used to simulate the Unit 2 accident [5] [6] [7] with uncertainties that exist in the modeling of the RCIC turbine. The uncertainties, (e.g., steam nozzle size for instance) are being investigated by running multiple simulations. Striking in these simulations is the cooled condition of the reactor system that persistently develops, as RCIC self-regulates to balance the water delivery capacity and steam consumption demands of the RCIC system against the fission product decay power in the reactor. The MELCOR model makes use of the turbine wheel bucket inlet and outlet velocities determined by the CFD analyses described in Section 4.

Results of the current best-estimate Fukushima Daiichi Unit 2 MELCOR simulation are presented and followed by discussions of known modeling uncertainties. In large part, resolution of the uncertainties is awaiting planned testing [8]. A shortcoming that exists is the simulation in that boiler pressure does not track recorded pressure in the accident especially well. Resolution of the modeling uncertainties is expected to remedy this shortcoming.

Figure 11 through Figure 14 present the current best-estimate MELCOR simulation of RCIC response in the Fukushima Daiichi Unit 2 accident where RCIC managed to cool the reactor for an extended period of time (~68 hours) without electricity available to power turbine's speed control system.

Boiler pressure in the current best-estimate Fukushima Daiichi Unit 2 simulation is shown in Figure 11 along with data recorded in the accident. Additionally, Figure 11 shows boiler pressure in a simulation assuming smaller steam nozzles than assumed in the best-estimate simulation (0.500" versus 0.584" diameter) to illustrate the level of uncertainly in the simulations. The trend seems good in this figure but the offset of the simulations relative to the data suggests that RCIC is pumping too efficiently in the simulations. The strong depressurization occurring when backup electrical power is lost at 1-hour results from the large increase in RCIC flow to the reactor when the power loss causes the RCIC turbine control valve to open fully. The strong inflection at 1+ hour results from the RCIC turbine ingesting water once the RPV overfills to the MSL nozzles and spills into the MSLs. The inflection at ~11 hours is RCIC self-regulating to a higher pressure in response to the operators switching RCIC suction from the relatively cold CST to the hotter wetwell. The hotter water has less cooling capacity and so more of it is needed to cool the reactor. For RCIC to pump more water, steam pressure needs to be higher. The uncertainty in steam nozzle size shows to be large in the MELCOR simulations.

The RPV level is shown in Figure 12. RCIC tripping twice on high level before electrical power loss at 1-hour is also reflected in this figure. Level climbs rapidly when the RCIC turbine governor valve opens fully on loss of electrical power and overfills the RPV to the MSLs.

RCIC steam supply and exhaust pressure is shown in Figure 13. Note the large drop in pressure across the RCIC turbine control valve while the RCIC control system has electrical power and RCIC is operating normally. This pressure drop reduces markedly when the control valve opens fully on loss of electrical power at 1-hour.

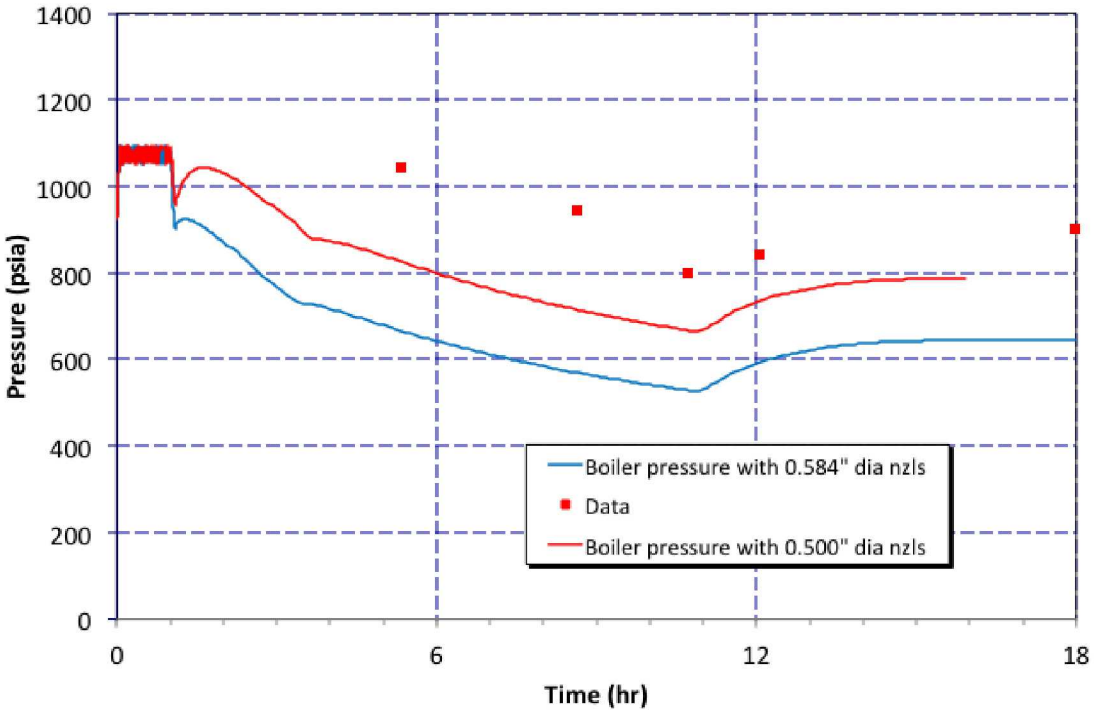

Figure 11. Simulated Fukushima Daiichi Unit 2 Boiler Pressure

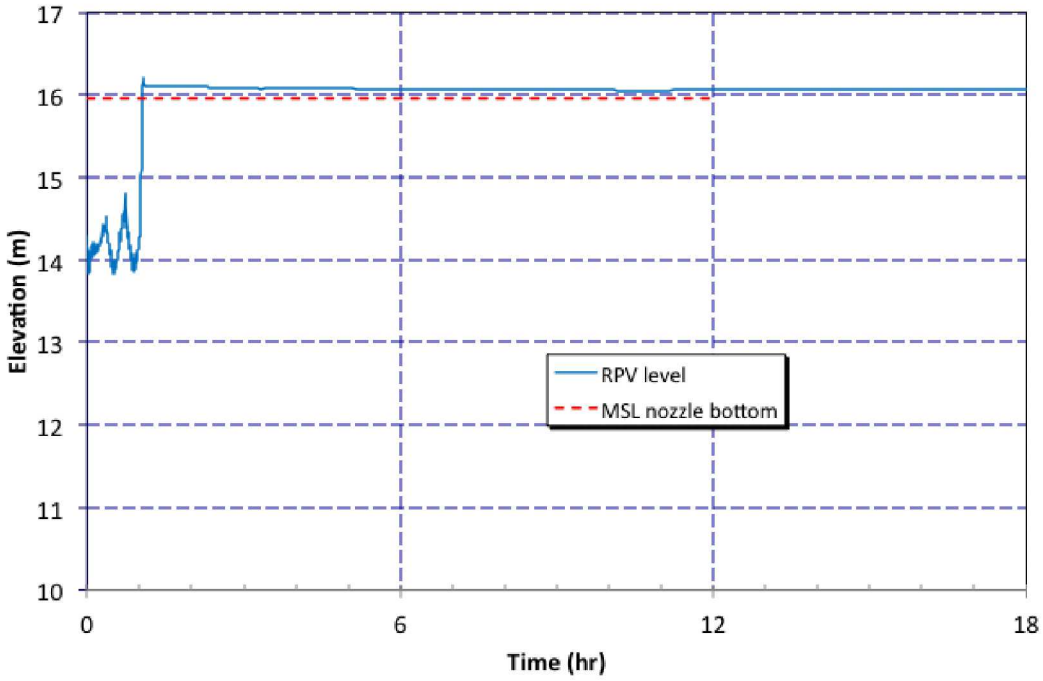

Figure 12. Simulated Fukushima Daiichi Unit 2 RPV Level

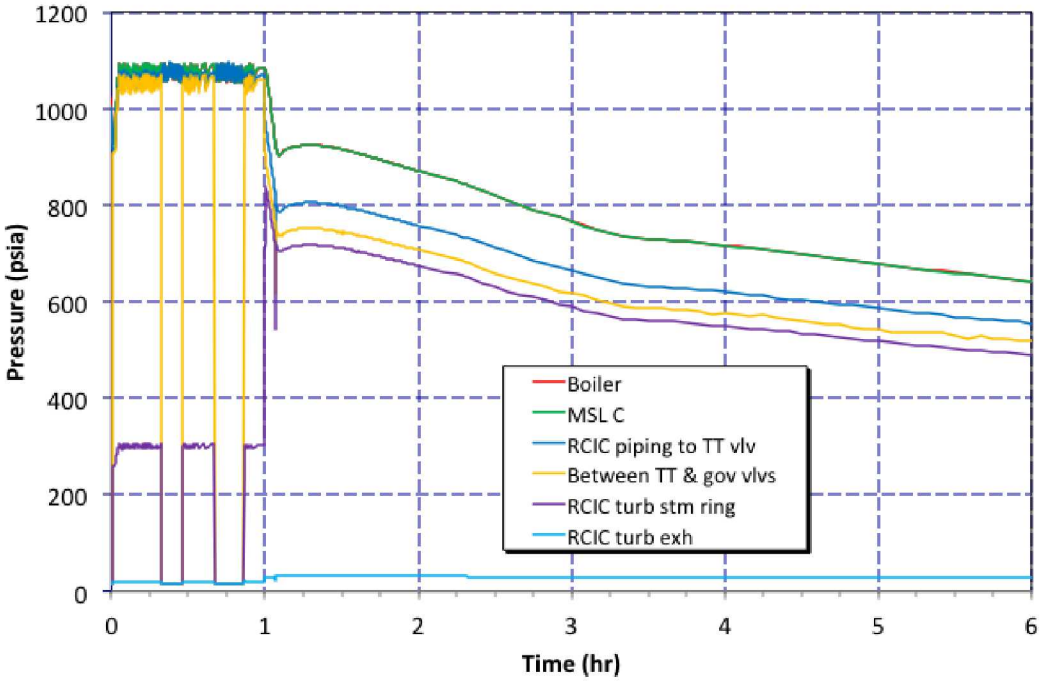

Figure 13. Simulated Fukushima Daiichi Unit 2 Steam Pressure

RCIC speed is shown in Figure 14. The RCIC turbine governor valve opening fully on loss of electrical power sends RCIC speed high enough to trip the turbine on overspeed. The indicated over-speed trip (green dashed line) was ignored (i.e., RCIC was allowed to continue to run). Water ingestion by the RCIC turbine at 1+ hour brings RCIC speed back down. The inflection at ~11 hours is RCIC's self-regulating response to the operators switching RCIC suction from the CST to the wetwell.

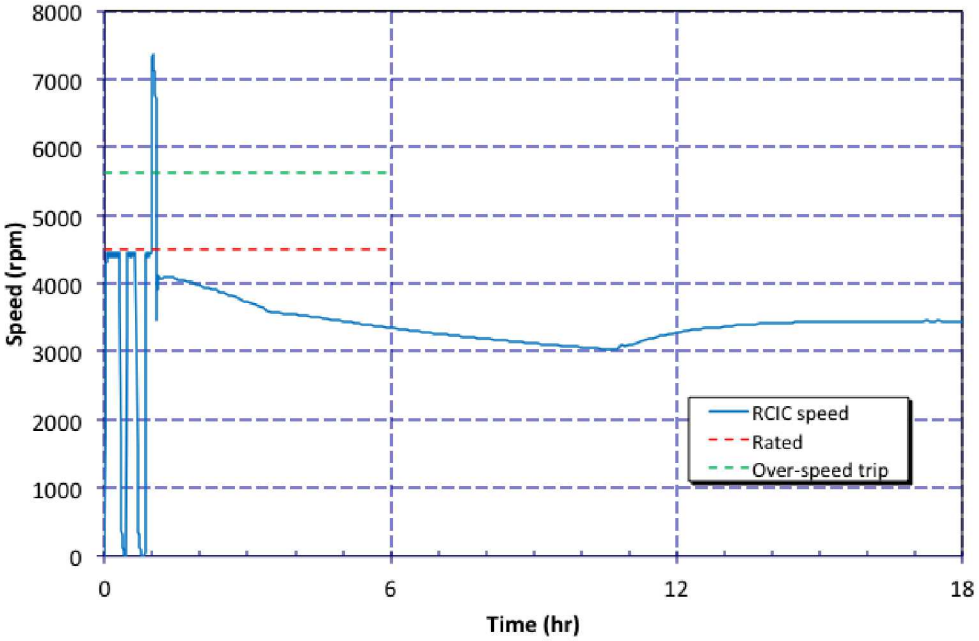

Figure 14. Simulated Fukushima Daiichi Unit 2 RCIC Speed

The self-regulating condition suspected of developing in the Fukushima Daiichi Unit 2 accident where RCIC stably cooled the reactor for an extended period of time without electrical power is being convincingly demonstrated in current MELCOR modeling. The lack of electrical power in the accident meant that RCIC's normal speed control system was not active and that RCIC's turbine governor valve was fully open. As suggested in the MELCOR calculations, RCIC overfilled the reactor vessel to where water spilled into the steam lines and hence was ingested by the RCIC turbine. Water collected in the RCIC turbine steam ring effectively blocking some number of the 5 installed steam nozzles from flowing steam. This blocking is how RCIC managed to modulate itself. If RCIC water delivery to the reactor was too large, relative to what was needed for a balanced situation, the amount of water content in the steam ring rose blocking more nozzles to steam flow and RCIC water delivery fell. If RCIC water delivery to the reactor was too small, the amount of water in the steam ring dropped opening more nozzles to steam flow and water delivery rose.

It is important to note that MELCOR separates phases by default and so develops a water pool low in the steam ring and a steam atmosphere high in the ring; nozzles low in MELCOR steam ring block with water. The realism of the phase separation in the steam ring exhibited by MELCOR is presently unknown but separation of liquid and steam phases in the stream ring does show in cursory SNL CFD calculations [7]. The degree of phase separation the steam rings is another uncertainty in the MELCOR calculation. Notable is that changes to uncertain parameters in the RCIC representation in the MELCOR model that altered the efficiency of the turbine simply caused the amount of water in the turbine steam ring to go up or down to re-achieve a balanced situation.

Why the RCIC system in the Fukushima Daiichi Unit 2 accident did not trip on over-speed remains a confounding question. When electrical power to the RCIC speed control system was lost, the turbine steam-governing valve would have fully opened and would have happened with the reactor at full pressure. Consensus industry understanding is that turbine speed would have increased rapidly at this point exceeding the mechanical overspeed trip setting and the RCIC turbine stop valve would have closed. This would have stopped the RCIC system but clearly this did not happen. Why remains inexplicable.

6. NEW MELCOR TERRY TURBINE MODELING OPTION

The modeling of the Fukushima Daiichi Unit 2 RCIC turbine in the MELCOR calculations described in Section 5 was accomplished using an involved collection of control functions that capture the basic principles of Terry turbine operation. The same modeling can now be accomplished relatively simply using a newly incorporated MELCOR option that allows the user to include an impulse turbine-driven pump in a model without describing how it operates [9]. Specifics of the inner workings of the new MELCOR option follow in the subsections.

6.1. Terry Turbine Velocity Stage Model

The Terry turbine compound velocity stage model in MELCOR is based on angular momentum balance over a turbine control volume. The model explicitly accounts for:

- Several separate nozzles and their jets of steam/water
- Optionally, noncondensable gas as a substitute for steam
- Each bucket/reversing chamber pair (i.e. each velocity stage)
- A general number 'n' of reversing chambers allotted per steam nozzle, with the proposed capability to model any user-requested number of steam nozzles that may be circumferentially-situated about the rotor wheel

The quantity of interest in a velocity stage model of an impulse-type turbine is the momentum flux delivered to the rotor because the attending force ultimately turns the rotor and exerts a "positive" torque on a coupled shaft. For a compounded velocity stage, the total momentum flux and/or force integrated over all velocity stages must be computed. The MELCOR Terry turbine velocity stage model predicts a turbine torque that is intended to factor into a shaft torque/inertia (angular speed) equation which dictates pump impeller speed and hence turbopump performance.

6.2. Terry Turbine Pressure Stage Model

The pressure stage model treats the flow of steam (dry saturated or superheated) or noncondensable gas through a converging/diverging nozzle. Isentropic single-phase flow is assumed for the case of noncondensable gas flow. For steam flow, a sequence of expansion processes is assumed:

- An isentropic expansion from the nozzle inlet through the throat and to a point where condensation heat release begins to introduce entropy
- A Rayleigh flow process between the end of the last isentropic expansion and the Wilson point (point of maximum nucleation, maximum steam super-saturation)
- A Rayleigh flow process between the Wilson point and the point of full reversion from thermodynamic non-equilibrium (re-establishment of saturation)
- An isentropic expansion between the end of the last Rayleigh flow process and the nozzle outlet with provision for standing normal shocks
- A standing normal shock (over-expanded flow with respect to back-pressure) or a jet expansion (if under-expanded flow with respect to back-pressure)

The steam expansion process (disregarding aerodynamic shocks) is shown in Figure 15. The states included on the h-s (enthalpy-entropy) diagram are:

- **01**, representing inlet stagnation conditions
- **2**, representing the point where expanding steam crosses the saturation line
- **m**, representing the point where condensation starts to release latent heat to the steam such that significant entropy is introduced
- **n**, representing the Wilson point (point of maximum nucleation and maximum super-saturation), reached at a time t_n after point 2 is reached
- **a**, representing the state that expanding steam would have reached if it expanded on an isentropic line for a time t_n after point 2 is reached
- **3**, representing the point where thermodynamic phase equilibrium is re-established
- **4**, representing the nozzle exit state (on an isentropic line with state 3, no shocks)

The only distinguishing feature from conventional isentropic compressible flow theory is the latent heat release between states **m** and **3**. This process can be modeled by a Rayleigh flow process which assumes:

- One dimensional flow through a constant cross-sectional area duct
- Steady flow
- Frictionless flow
- Heat addition (non-adiabatic flow)

In the present case, thermal energy is added to flowing steam due to latent heat release. Heat addition in this case equals the product of latent heat and wetness fraction. Thus, the heat addition is proportional to evolved wetness which can be obtained by evaluation of the so-called nucleation-growth integrals. Rayleigh flow relationships are such that a downstream state (e.g. state '**n**') can be determined from an upstream state (idealized state '**a**' in this case) and a known heat addition between the two states.

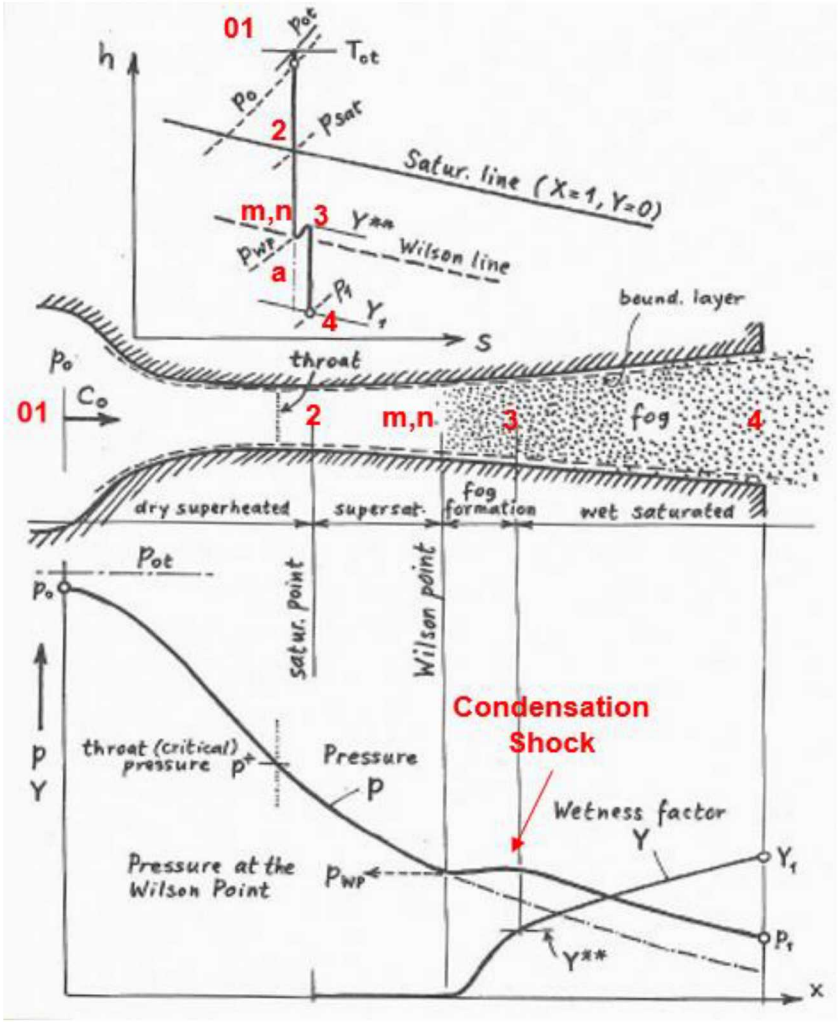

Figure 15. Qualitative h-s Diagram and Pressure/Wetness Plots for Steam Expansion [9]

An ideal gas equation-of-state relationship is typically chosen for analytical Wilson point solutions, and this assumption has been shown to compare well with more rigorous computations and experiments. Assumption of a purely isentropic steam expansion (to the neglect of any steam phase metastability) is an alternate strategy to the analytical Wilson point approach. Both formulations are discussed in Section 6.3 and Section 6.4, respectively.

6.3. Steam Nozzle Expansion Model

A strategy for "marching" through the one-dimensional, steady, frictionless ideal gas converging-diverging nozzle steam flow was developed. Concepts of isentropic flow and Rayleigh flow are applied for different segments of the nozzle. Reference is made to Figure 15 as its state points (**01**, **2**, **m**, **n**, **a**, **3**, **4**) are treated as "expansion waypoints" that guide the expansion model calculation. The process is outlined in subsequent paragraphs for each step to computing steam nozzle expansion.

First, a stagnation state **01** is fixed from known CV conditions upstream of the nozzle FL and from assumed specific heat ratio $\gamma = 1.3$ or 1.14 for superheated or saturated steam, respectively. The relationships are purely algebraic and require no iteration to solve.

Second, the saturated state **2** is fixed using known conditions at **01**, isentropic flow relations, and a saturation line equation. A system of two equations are solved with a Newton iteration scheme. If no solution is found for a given set of nozzle inlet conditions, an isentropic expansion of steam (superheated throughout expansion) is assumed through the nozzle.

Third, states **a** and **n** are solved with an iterative technique. This "wetness iteration" attempts to arrive at a self-consistent set of conditions for the isentropic reference state **a** and the Wilson point **n** according to a highly non-linear set of equations that encapsulate all applicable isentropic flow, Rayleigh flow, and nucleation/growth relationships. Mathematical details of the process are omitted in favor of a qualitative description. The solution procedure involves a Regula-Falsi search for a Wilson point temperature that leads to convergence of nucleation pulse half-width as predicted by two separate prescriptions. The converged nucleation pulse half-width yields Wilson point wetness directly and thereby all state **a** and **n** properties. At the end of each wetness iteration, the updated state properties at **a** and **n** including wetness are checked to judge convergence and self-consistency in results. If the searching algorithm and Regula-Falsi solution method cannot establish a Wilson point temperature leading to sufficiently converged nucleation pulse half-width, metastability is discounted and an isentropic steam expansion from state **2** to state **4** is assumed.

Fourth, a Rayleigh flow process is followed from the Wilson point **n** to the reversion point **3** which is the point where saturation conditions are re-established. Four equations are iteratively solved. If no solution is found during the Newton's method system solve, an assumption of thermally-choked flow is applied. In this case, the latent heat released during reversion from the Wilson point is sufficient to either:

- Lower the Mach number to unity if M_n was larger than unity, or
- Raise the Mach number to unity if M_n was smaller than unity

This behavior is consistent with the nature of the "Rayleigh line" which the Rayleigh flow process follows from **n** to **3**. The choked Rayleigh flow property relations and a special entropy equation may be applied in this case where the Mach number at state **3** is unity.

Fifth, a specialized homogeneous-equilibrium two-phase flow model is employed to model the expansion of saturated steam between states **3** and **4**. A two-phase mixture of an ideal gas and a dilute, dispersed secondary phase may be treated with the conventional HEM plus augmented specific heats depending on the mass fraction of the dispersed phase. This approach holds under the assumption of thermal equilibrium between the continuous gas phase and dilute liquid phase (as would occur under saturation conditions). Thus, the pseudo-gas is treated as ideal but with modified specific heat and specific heat ratio. To get to state **4**:

- A Newton's method solution to an ideal gas expansion law and the saturation line equation is done to recover pressure and temperature at state **4**
- A Newton's method solution to a stagnation pressure relation is used to get the Mach number at state **4**
- A Newton's method solution to a stagnation enthalpy relation is used to compute the wetness at state **4**

Sixth, if an oblique shock ought to exist according to turbine back pressure (i.e. if over-expansion occurs such that state **4** pressure is lower than the back pressure), the effects of such a phenomenon are approximated by those of a standing normal shock and are imposed on the nozzle outlet state **4**. If instead the flow at state **4** is under-expanded (i.e. if pressure at state **4** is higher than the back pressure), an algebraic formulation proposed by Idaho National Laboratory is used to predict the jet expansion that occurs between the nozzle outlet plane and the rotor bucket inlet. The model is based on the "virtual nozzle" concept. Three sequentially-solved algebraic equations are used to predict:

- Velocity and Mach number at end of virtual nozzle
- Temperature at end of virtual nozzle (pressure is known turbine back pressure)
- Density at end of virtual nozzle

The nozzle outlet conditions feed into the Terry turbine compound velocity stage model so that impulses delivered by steam on the turbine can be calculated.

6.4. Ideal, Isentropic Steam Expansion

The solution process for steam expansion assuming ideal, isentropic flow is:

- Using the assumed critical pressure ratio, get nozzle throat conditions
- Compute the state **4** properties from throat properties and user-input area fraction (nozzle exit to nozzle throat) using an iterative bisection approach
- Compute a normal shock or jet expansion depending on back pressure

7. CONCLUSIONS

Efforts are being pursued to qualify a system-level model of a RCIC/TDAFW steam turbine-driven pump. The model is being developed with the intent of employing it to inform the design of experimental configurations for full-scale Terry turbine testing [8]. The model is expected to be especially valuable in sizing equipment needed for this testing. An additional intent is to use the model in understanding more fully how RCIC apparently managed to operate far removed from its design envelope in the Fukushima Daiichi Unit 2 accident.

This modeling is proceeding along two avenues that are expected to complement each other well. The first avenue is the continued development of the system-level (RCIC and TDAFW) model that will serve in simulating a full reactor system or full experimental configuration of which a Terry turbopump is part. The models reasonably represent a RCIC/TDAFW system today, especially given design operating conditions, but lacks specifics that are likely important in representing the off-design conditions the system might experience in a beyond design basis situation such as an extended loss of all electrical power. A known specific lacking in the system model, for example, is the efficiency at which a flashing slug of water (as opposed to a concentrated jet of steam) could propel the rotating drive wheel of a RCIC turbine. To address this specific example, a second avenue is being pursued wherein CFD analyses of such a jet are carried out. The results of the CFD analyses will thus complement and inform the system modeling. The system modeling will, in turn, complement the CFD analysis by providing the system information needed to impose appropriate boundary conditions on the CFD simulations. The system model will be used to inform the selection of configurations and equipment best suitable of supporting planned experimental testing [8].

ACKNOWLEDGMENTS

This endeavor is the product of and supported by a group of people representing several organizations. This includes the US Department of Energy; the Japanese Ministry of Economy, Trade, and Industry; the Boiling Water Reactor Owners Group; Sandia National Laboratories; Idaho National Laboratory; The Institute of Applied Energy; Texas A&M University; US and Japanese utilities; US and Japanese vendors; and others.

REFERENCES

1. R. Gauntt et al., "Fukushima Daiichi Accident Study (Status as of April 2012)," SAND2012-6173, Sandia National Laboratories, Albuquerque, NM, USA (2012).
2. D. Osborn, M. Solom, K. Ross, K. Kirkland, A. Patil, and N. Tsuzuki, "Terry Turbine Expanded Operating Band: Initial Experimental Efforts," *in preparation for submittal to the* 2018 ANS Winter Meeting Embedded Topical on Advances in Thermal Hydraulics (ATH 2018), Orlando, FL, USA, November 11-15, 2018.
3. C.W. Dyson, "Test of Terry Steam Turbine," *Journal of the American Society of Naval Engineers*, **21** (3), pp. 884-890 (1909).
4. Author Unknown, "The Terry Turbine-Driven Fans," *Journal of the American Society of Naval Engineers*, **30** (3), pp. 598-599 (1918)
5. K. Ross et al., "Modeling of the Reactor Core Isolation Cooling Response to Beyond Design Basis Operations – Phase 1," SAND2015-10662, Sandia National Laboratories, Albuquerque, NM, USA (2015).
6. K. Ross, J. Cardoni, and D. Osborn, "Terry Turbopump Analytical Modeling Efforts in Fiscal Year 2016 – Progress Report," SAND2018-4337, Sandia National Laboratories, Albuquerque, NM, USA (2018).
7. J. Cardoni, K. Ross, and D. Osborn, "Terry Turbopump Analytical Modeling Efforts in Fiscal Year 2017 – Progress Report," SAND2018-4533, Sandia National Laboratories, Albuquerque, NM, USA (2018).
8. D. Osborn, M. Solom, K. Ross, and J. Cardoni, "Terry Turbopump Expanded Operating Band Full-Scale Component Experiments and Basic Science Detailed Test Plan – Revision 2," SAND2017-10773, Sandia National Laboratories, Albuquerque, NM, USA (2017).
9. B Beeny, "Computational Multiphase Fluid Dynamics Analyses and Systems-Level Model Development for a Reactor Core Isolation Cooling System Terry Turbine," PhD Dissertation, Texas A&M University, College Station, TX, USA (2017).